

Accepted manuscript

Garcia, A. S., Kristensen, S. T. & Strandberg, R. (2022). Analytical Modeling of the Temperature Sensitivity of the Maximum Power Point of Solar Cells. IEEE Journal of Photovoltaics, 12(5), 1237-1242. <https://doi.org/10.1109/JPHOTOV.2022.3178175>

Published in: IEEE Journal of Photovoltaics

DOI: <https://doi.org/10.1109/JPHOTOV.2022.3178175>

AURA: <https://hdl.handle.net/11250/3063590>

Copyright: © 2022 IEEE

© 2022 IEEE. Personal use of this material is permitted. Permission from IEEE must be obtained for all other uses, in any current or future media, including reprinting/republishing this material for advertising or promotional purposes, creating new collective works, for resale or redistribution to servers or lists, or reuse of any copyrighted component of this work in other works.

Analytical Modeling of the Temperature Sensitivity of the Maximum Power Point of Solar Cells

Alfredo Sanchez Garcia, Sissel Tind Kristensen, and Rune Strandberg
University of Agder, Grimstad, 4879, Norway

Abstract

This work presents new analytical expressions for the temperature coefficients of the voltage, current and power of a solar cell at its maximum power point. A new analytical expression of the temperature coefficient of the fill factor is also derived. The new expressions are written as functions of solar cell parameters that can be extracted from the current-voltage characteristic of the cell. Non-ideal diode behavior is partially accounted for through a temperature dependent ideality factor. The recombination parameter γ , which has been shown to account for the thermal sensitivity of all mechanisms determining the open-circuit voltage, appears to play a role also for the temperature coefficient of the maximum power point. The expressions are tested against experimental data, which covers measurements from 18 multicrystalline silicon solar cells with different bulk resistivities and cell architectures. It is found that the new model captures the essence of the temperature variation shown by the investigated parameters.

1 Introduction

The temperature sensitivity of a solar cell parameter, such as the open-circuit voltage, V_{oc} , is usually described by its temperature coefficient (TC) [1]. Some work has been done aiming to explicitly quantify the TCs of V_{oc} and the short-circuit current, i_{sc} [2, 3], but so far, there has not been much focus on the temperature sensitivity of the maximum power point (MPP). Quantification of TCs, particularly at the MPP, is of special importance as it is desirable to accurately predict the temperature dependent performance of solar cells under real operating conditions. The lack of

analytical models describing the temperature sensitivity of the MPP represents a gap in the scientific literature which this work seeks to fill. To this end, Khanna’s model for the maximum power point [4] is used as a starting point to derive analytical expressions for the TCs of the voltage, current and power at the MPP. Inspired by the work of Dupré et al. in Ref. [3], the influence of the recombination parameter γ in the temperature sensitivity of the MPP is also explored. For this, energy losses related to non-radiative recombination are considered through the *External Radiative Efficiency* (ERE), as defined in Ref. [5]. The derived expressions also account for temperature variations of the bandgap, which are modeled with a linear function of the temperature. Some preliminary results have already been presented in Ref. [6]. This extended version includes the derivation of the expressions for the TCs of photovoltaic parameters that were not included in the preliminary version. In the present work, non-ideal diode behavior is also accounted for through a temperature dependent ideality factor. The derived quantities are expressed as functions of each other and of well-known parameters, such as V_{oc} and i_{sc} . This allows for the derivation of an analytical expression for the TC of the fill factor. Finally, the new expressions are tested with experimental data obtained from suns- V_{oc} measurements of 18 multicrystalline silicon solar cells with different bulk resistivities and cell architectures.

2 Theoretical Background

Assuming non-degenerate conditions, the total current density, i , produced by a solar cell as a function of its voltage V , is given by Shockley’s diode equation [7],

$$i = i_G - i_0 \exp\left(\frac{V}{mV_t}\right) \approx i_{sc} - i_0 \exp\left(\frac{V}{mV_t}\right), \quad (1)$$

where i_0 is the thermal recombination current [8] and the photogeneration current, i_G , has been approximated by the short-circuit current, i_{sc} . This assumption is valid for practically all solar cells [9]. The *thermal voltage* V_t is defined by $qV_t = kT$, where k is Boltzmann’s constant and T is the cell temperature. Non-ideal diode behavior is accounted for through the ideality factor m which is assumed to be constant with respect to the voltage but allowed to vary with the temperature. As commonly found in literature on solar cells, the open-circuit voltage V_{oc} is easily obtained from Eq. (1) by setting $i = 0$, which gives

$$V_{oc} = mV_t \log\left(\frac{i_{sc}}{i_0}\right). \quad (2)$$

The power P delivered by the cell is given by the product $P = Vi$ [9]. At the maximum power point, it holds that $dP/dV = 0$. In Ref [4], Khanna et al. found that Lambert's W function, defined by $z = W(ze^z)$ [10], allows for an analytical expression of the maximum power point voltage, V_{mpp} , of the form

$$\begin{aligned} V_{\text{mpp}} &= mV_t \left[W \left(e^{\frac{i_{\text{sc}}}{i_0}} \right) - 1 \right] \\ &= mV_t \left[W \left(e^{1+V_{\text{oc}}/mV_t} \right) - 1 \right], \end{aligned} \quad (3)$$

where Eq. (2) was made use of in order to write $i_{\text{sc}}/i_0 = \exp[V_{\text{oc}}/mV_t]$. The maximum power point current, i_{mpp} , is obtained by inserting Eq. (3) into Eq. (1). This yields

$$i_{\text{mpp}} = i_{\text{sc}} \left[1 - \frac{1}{W \left(e^{1+V_{\text{oc}}/mV_t} \right)} \right]. \quad (4)$$

The maximum power that a solar cell can produce is given by [9]

$$P_{\text{mpp}} = V_{\text{mpp}}i_{\text{mpp}} = V_{\text{oc}}i_{\text{sc}}\text{FF}, \quad (5)$$

where FF is the *Fill Factor*. Inserting Eqs. (3) and (4) yields [4, 11]

$$P_{\text{mpp}} = mV_t i_{\text{sc}} \left[W \left(e^{1+V_{\text{oc}}/mV_t} \right) - 2 + \frac{1}{W \left(e^{1+V_{\text{oc}}/mV_t} \right)} \right]. \quad (6)$$

2.1 Temperature Coefficient

The TC of a solar cell parameter ($V_{\text{oc}}, i_{\text{sc}} \dots$) describes how this parameter changes with the temperature. The *relative temperature coefficient* of a parameter, X , as a function of the temperature, T , denoted here $\beta_X^r(T)$, is defined as the rate of change of X over the considered temperature range and normalized by X , i.e., [12]

$$\beta_X^r(T) = \frac{1}{X} \frac{dX}{dT} = \frac{d}{dT} \log [X(T)]. \quad (7)$$

The temperature dependence of many solar cell parameters, such as V_{oc} or the efficiency, is approximately linear for normal operating temperatures [1]. The derivative in Eq. (7) is then nearly constant and the temperature coefficient becomes a single valued parameter, hence its designation. Inserting Eq. (5) in Eq. (7), it is seen that the relative TC of P_{mpp} can be expressed as the sum of the relative TCs of $V_{\text{oc}}, i_{\text{sc}}$ and FF, i.e., [3]

$$\beta_{P_{\text{mpp}}}^r = \beta_{V_{\text{oc}}}^r + \beta_{i_{\text{sc}}}^r + \beta_{\text{FF}}^r = \beta_{V_{\text{mpp}}}^r + \beta_{i_{\text{mpp}}}^r. \quad (8)$$

2.2 The recombination parameter γ

For a solar cell operating at the radiative limit, the thermal recombination current, i_0 in Eq. (1), is well approximated by

$$i_0 \approx qV_t \exp\left(-\frac{E_g}{qV_t}\right) E_g^2. \quad (9)$$

To account for non-radiative recombination, Green introduced the concept of External Radiative Efficiency (ERE) in Ref. [5]. The ERE is defined as *the fraction of the total dark current recombination in the cell that results in radiative emission from the cell* [5]. Following Ref. [3], the ERE is introduced in Eq. (1) by making the substitution $i_0 \rightarrow i_0/\text{ERE}$. Assuming that the ERE is independent on the voltage, the expression for V_{oc} in Eq. (2) becomes

$$V_{oc} = V_t \log\left(\text{ERE} \frac{i_{sc}}{i_0}\right), \quad (10)$$

where m is set to 1 to match the expression presented in Ref. [3]. Using Eqs. (10) and (7) as a starting point, it can be shown that the *absolute TC* of V_{oc} , $\beta_{V_{oc}}$, is given by [3]

$$\beta_{V_{oc}} = \frac{V_{oc} - \frac{E_{gc}}{q} - \frac{kT}{q}\gamma}{T}, \quad (11)$$

with

$$\gamma = 1 + 2T \frac{E'_g}{E_g} - T \frac{\text{ERE}'}{\text{ERE}} - T \frac{i'_{sc}}{i_{sc}}, \quad (12)$$

where the prime denotes derivative with respect to the temperature. This explicit expression for the γ parameter is obtained by making use of the explicit form of i_0 found in Eq. (9). To obtain Eqs. (11) and (12), one also needs to assume a bandgap that changes linearly with the temperature [1], i.e.,

$$\begin{aligned} E_g(T) &\approx E_g(T_c) + (T - T_c) \left. \frac{dE_g}{dT} \right|_{T=T_c} + \mathcal{O}(T^2) \\ &= E_{gc} + TE'_g + \mathcal{O}(T^2), \end{aligned} \quad (13)$$

with $E_{gc} = E_g(T_c) - T_c E'_g$. For, e.g., crystalline silicon, $E_{gc} = 1.206$ eV and $E'_g = -2.73 \times 10^{-4}$ eVK⁻¹ [1]. The recombination parameter γ in Eq. (12) was first introduced by Green in Ref. [1] as a way to account for the temperature sensitivity of all mechanisms determining V_{oc} and was later explicitly quantified by Dupré et al. in Ref. [3]¹.

¹The notation $T \frac{X'}{X}$ is equivalent to $\frac{d \log X}{d \log T}$.

3 The model

To shorten the notation, the argument of Lambert's W function in Eqs. (3), (4) and (6) is denoted by z_{oc} . Foreseeing its usability in the coming derivations, note from Eq. (4) that

$$\frac{1}{W(z_{oc})} = 1 - \frac{i_{mpp}}{i_{sc}}. \quad (14)$$

This identity will be used in the derivation of the expressions for the TCs to eliminate the W functions when this is advantageous. From Eqs. (3) and (7), the relative TC of V_{mpp} , $\beta_{V_{mpp}}^r$, is given by

$$\begin{aligned} \beta_{V_{mpp}}^r &= \frac{d}{dT} \log V_{mpp} \\ &= \frac{d}{dT} \log [mV_t [W(e^{1+V_{oc}/V_t}) - 1]] \\ &= \frac{1}{T} + \frac{m'}{m} + \frac{1}{W(z_{oc}) - 1} \frac{d}{dT} W(z_{oc}) \\ &= \frac{1}{T} + \frac{m'}{m} + \frac{1}{W(z_{oc}) - 1} \frac{W(z_{oc})}{1 + W(z_{oc})} \frac{d}{dT} \left[1 + \frac{V_{oc}}{V_t} \right] \\ &= \frac{1}{T} + \frac{m'}{m} + \frac{mV_t}{V_{mpp}} \frac{W(z_{oc})}{1 + W(z_{oc})} \frac{d}{dT} \left[1 + \frac{V_{oc}}{mV_t} \right], \end{aligned} \quad (15)$$

where the derivative of Lambert's W function, which can be found in, e.g., Ref. [10] was used. Additionally, Eq. (3) was used to make $(W(z_{oc}) - 1)^{-1} = mV_t/V_{mpp}$. The last derivative in Eq. (15) can be written as

$$\begin{aligned} \frac{d}{dT} \left[1 + \frac{V_{oc}}{mV_t} \right] &= \frac{dV_{oc}}{dT} \frac{q}{mkT} - \frac{qV_{oc}}{mkT^2} - \frac{m'}{m} \\ &= \frac{V_{oc}}{mV_t} \left[\beta_{V_{oc}}^r - \frac{1}{T} - \frac{m'}{m} \right], \end{aligned} \quad (16)$$

where the definitions of relative TC in Eq. (7) was used. Inserting now Eq. (16) into the last line of Eq. (15) yields

$$\beta_{V_{mpp}}^r = \frac{1}{T} + \frac{m'}{m} + \frac{W(z_{oc})}{1 + W(z_{oc})} \left[\beta_{V_{oc}}^r - \frac{1}{T} - \frac{m'}{m} \right] \frac{V_{oc}}{V_{mpp}}. \quad (17)$$

Employing Eq. (14) to eliminate the W functions, the factor in front of the parenthesis of Eq. (17) becomes

$$\frac{W(z_{oc})}{1 + W(z_{oc})} = \frac{i_{sc}}{2i_{sc} - i_{mpp}} = \mathcal{I}. \quad (18)$$

To shorten the notation, note that $1/T + m'/m$ equals the derivative with respect to the temperature of the logarithm of mV_t , i.e., $\beta_{mV_t}^r$. Eq. (17) then becomes

$$\beta_{V_{\text{mpp}}}^r = \beta_{mV_t}^r + \mathcal{I} [\beta_{V_{\text{oc}}}^r - \beta_{mV_t}^r] \frac{V_{\text{oc}}}{V_{\text{mpp}}}. \quad (19)$$

Performing the same type of derivation with Eqs. (4) and (6) as starting points, the relative TCs of i_{mpp} and P_{mpp} can be expressed as

$$\beta_{i_{\text{mpp}}}^r = \beta_{i_{\text{sc}}}^r + (1 - \mathcal{I}) [\beta_{V_{\text{oc}}}^r - \beta_{mV_t}^r] \frac{V_{\text{oc}}}{V_{\text{mpp}}}, \quad (20)$$

$$\beta_{P_{\text{mpp}}}^r = \beta_{mV_t}^r + \beta_{i_{\text{sc}}}^r + [\beta_{V_{\text{oc}}}^r - \beta_{mV_t}^r] \frac{V_{\text{oc}}}{V_{\text{mpp}}}, \quad (21)$$

where it is straightforward to show that Eqs. (19), (20) and (21) satisfy Eq. (8). Finally, using Eqs. (8) and (21), the relative TC of the fill factor, FF, can be written as

$$\begin{aligned} \beta_{\text{FF}}^r &= \beta_{P_{\text{mpp}}}^r - \beta_{V_{\text{oc}}}^r - \beta_{i_{\text{sc}}}^r \\ &= \beta_{mV_t}^r - (\beta_{mV_t}^r - \beta_{V_{\text{oc}}}^r) \frac{V_{\text{oc}}}{V_{\text{mpp}}} - \beta_{V_{\text{oc}}}^r \\ &= (\beta_{mV_t}^r - \beta_{V_{\text{oc}}}^r) \left(1 - \frac{V_{\text{oc}}}{V_{\text{mpp}}}\right). \end{aligned} \quad (22)$$

4 The recombination parameter γ

As mentioned in section 2, Green introduced the recombination parameter γ as a way to account for the temperature sensitivity of all mechanisms determining V_{oc} [9]. Eqs. (3), (4) and (6) show a direct link between the open-circuit voltage and the maximum power point. The parameter γ should therefore be expected to play a role in the temperature sensitivity of the maximum power point. In this section, the expressions for the TCs are derived in an alternative way to include the γ parameter. To match Dupré's expression in Ref. [3], $m = 1$ will be assumed in this section. By combining Eqs. (11) and (16), it becomes clear that

$$\frac{V_{\text{oc}}}{V_t} \left(\beta_{V_{\text{oc}}}^r - \frac{1}{T} \right) = \frac{1}{V_t} \left(\beta_{V_{\text{oc}}}^r - \frac{V_{\text{oc}}}{T} \right) = -\frac{1}{T} \left(\gamma + \frac{E_{\text{gc}}}{kT} \right), \quad (23)$$

with γ being given by Eq. (12). Substituting this identity into Eq. (17) yields

$$\begin{aligned}\beta_{V_{\text{mpp}}}^r &= \frac{1}{T} - \frac{W(z_{\text{oc}})}{1 + W(z_{\text{oc}})} \frac{1}{W(z_{\text{oc}}) - 1} \frac{V_{\text{oc}}}{V_t} \left[\frac{1}{T} - \beta_{V_{\text{oc}}}^r \right] \\ &= \frac{1}{T} - \frac{W(z_{\text{oc}})}{1 + W(z_{\text{oc}})} \frac{1}{W(z_{\text{oc}}) - 1} \frac{-1}{T} \left(\gamma + \frac{E_{\text{gc}}}{kT} \right) \\ &= \frac{1}{T} \left[1 + \frac{i_{\text{sc}}(i_{\text{sc}} - i_{\text{mpp}})}{i_{\text{mpp}}(i_{\text{mpp}} - 2i_{\text{sc}})} \left(\gamma + \frac{E_{\text{gc}}}{kT} \right) \right],\end{aligned}\quad (24)$$

where Eq. (14) has been used to eliminate the W functions. Likewise with $\beta_{i_{\text{mpp}}}^r$ and $\beta_{P_{\text{mpp}}}^r$, inserting Eq. (23) into (20) and (21) yields

$$\beta_{i_{\text{mpp}}}^r = \frac{1}{T} \left[T \frac{i'_{\text{sc}}}{i_{\text{sc}}} + \frac{(i_{\text{sc}} - i_{\text{mpp}})^2}{2i_{\text{sc}}i_{\text{mpp}} - i_{\text{mpp}}^2} \left(\gamma + \frac{E_{\text{gc}}}{kT} \right) \right], \quad (25)$$

$$\beta_{P_{\text{mpp}}}^r = \frac{1}{T} \left[1 + T \frac{i'_{\text{sc}}}{i_{\text{sc}}} + \left(1 - \frac{i_{\text{sc}}}{i_{\text{mpp}}} \right) \left(\gamma + \frac{E_{\text{gc}}}{kT} \right) \right]. \quad (26)$$

As for Eqs. (19), (20) and (21), it is straight forward to show that Eqs. (24), (25) and (26) also satisfy Eq. (8). Finally, it should be mentioned that alternative preliminary forms of Eqs. (24) and (25) were presented in Ref. [6].

5 Experimental Method

The theoretical expressions are compared to measurements of 18 solar cells with different bulk resistivities, ρ , and cell architectures. The cells are industrially fabricated from three different compensated p -type multi-crystalline silicon (mc-Si) ingots and can be divided into three groups: (a) $\rho = 1.3 \Omega \cdot \text{cm}$, *Aluminum Back Surface Field* (Al-BSF) cells, (b) $\rho = 0.5 \Omega \cdot \text{cm}$, *Passivated Emitter and Rear Cells* (PERC), (c) $\rho = 1.3 \Omega \cdot \text{cm}$, PERC. Each group contains six cells from various brick positions, numbered from 001-060, with position 001 denoting a cell from the bottom of the brick and position 060 denoting a cell from the top. The performance of the cells was measured with temperature dependent suns- V_{oc} using a NeonSeeTM AAA sun simulator with a built-in water heater. This allowed for the acquisition of $i - V$ data without series resistance effects at a temperature range between 293 K and 343 K, and subsequently, calculation of the TCs. The suns- V_{oc} method was chosen to enable better comparison with the theoretical expressions, which do not account for series resistance effects.

6 Numerical Method

From the temperature dependent suns- V_{oc} measurements, the experimental values of V_{oc} , i_{sc} , V_{mpp} , i_{mpp} , P_{mpp} and FF were extracted at multiple temperatures. The corresponding TCs were determined by fitting the measured values to second degree polynomials of the temperature before calculating the derivative at each of the measured temperatures. This method is chosen over a simpler linear regression because some of the measured solar cell parameters (particularly i_{sc} and i_{mpp}) show dependencies with the temperature that are far from linear. Regarding the temperature dependence of the ideality factor, Eq. (1) was evaluated at the MPP to obtain

$$m = \frac{1}{V_t} \frac{V_{mpp} - V_{oc}}{\log\left(1 - \frac{i_{mpp}}{i_{sc}}\right)}, \quad (27)$$

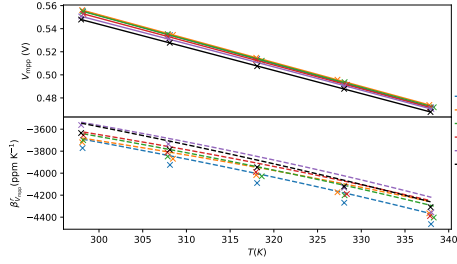
where Eq. (2) was used to eliminate i_G and i_0 . Note that m is voltage dependent for most common solar cells. This was also the case for the studied cells. If one assumes that $m(V)$ is not going to vary significantly from V_{mpp} to V_{oc} , Eq. (27) can be used to estimate m at the measured temperatures and then fit to a polynomial to obtain $m(T)$.

7 Experimental and numerical results

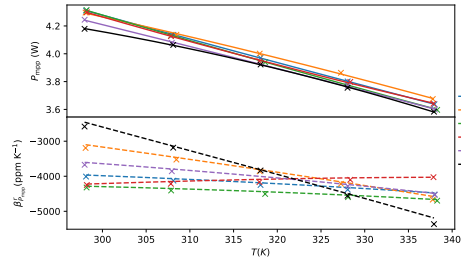
In this section, the polynomials of the temperature corresponding to the measured values of V_{oc} , i_{sc} , V_{mpp} , i_{mpp} , $\beta_{V_{oc}}^r$ and $\beta_{i_{sc}}^r$ are used to evaluate Eqs. (19), (20), (21) and (22). The obtained values are then compared to the experimental relative TCs, which are calculated according to the method explained in section 6.

Figs. 1, 2, and 3 present the numerical results as follows: In the upper graph of each subfigure, the parameter of interest is plotted as a function of the cell temperature. Here, the crosses represent measured values. For example, in the top graph of Fig. 1(a), the crosses correspond to the experimental values of V_{mpp} . The continuous lines display the polynomials that fit the measurements. Each color represents a cell from the ingot position stated in the legend. In the lower graph of each subfigure, the relative TC is plotted as a function of the cell temperature. Here, the experimental TCs are displayed with crosses. The dashed lines show the TCs calculated with the proposed model. In the bottom graph of, e.g., Fig. 1(a), the dashed lines display TCs calculated with Eq. (19).

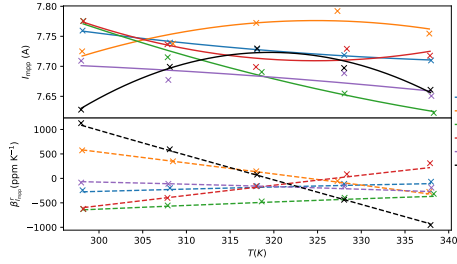
Starting with V_{mpp} , Figs. 1- 3(a) show a nearly linear dependence with the temperature for the measured cells. Eq. (19) describes reasonably well the measured



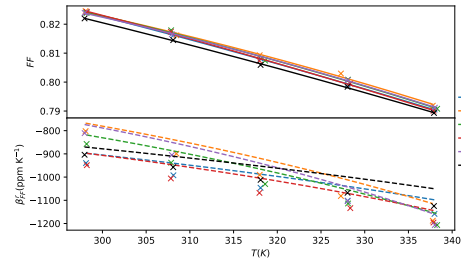
(a) V_{mpp} (top) and $\beta_{V_{mpp}}^r$ (bottom) as a function of the cell temperature.



(b) P_{mpp} (top) and $\beta_{P_{mpp}}^r$ (bottom) as a function of the cell temperature.



(c) i_{mpp} (top) and $\beta_{i_{mpp}}^r$ (bottom) as a function of the cell temperature.



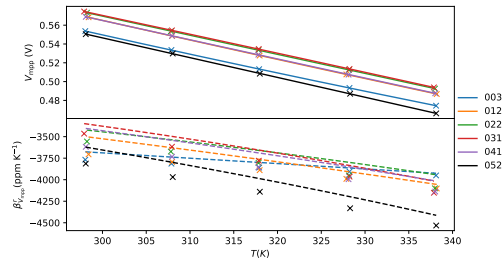
(d) FF (top) and β_{FF}^r (bottom) as a function of the cell temperature.

Figure 1: V_{mpp} , i_{mpp} , P_{mpp} , FF and their corresponding relative TCs as a function of the temperature for the cells in group (a). In all eight graphs, the experimental values and their TC are displayed with crosses. The continuous lines at the top graphs represent the polynomial fit of the measurements. The dashed lines at the bottom graphs correspond to the new expressions presented in this work.

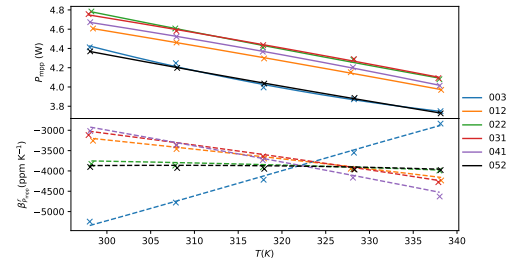
$\beta_{V_{\text{mpp}}}^r$ values, although discrepancies can be observed. In Fig. 1(a), the maximum discrepancy is of 3.2 %, found for the cell in position 022 at $T = 338$ K. A possible explanation for the discrepancies involves the possible non-ideal diode behavior of the measured cells. Some non-ideality is accounted for by the temperature dependent ideality factor, but this is still an approximation since the ideality factor in general may show some voltage dependency. Crystalline silicon cells are often better described with two-diode models rather than with Eq. (1). Noise in the measurements originating from the difficulties in stabilizing the temperature during the relatively long data acquisition times may also explain some of the discrepancy between the model and the experiments.

As for the temperature dependence of P_{mpp} , some small nonlinearities can be observed in Figs. 1- 3(b) (see, e.g., the curves corresponding to the cells in positions 022 and 044 at the in the top graph of Fig. 1(b)) but the overall dependence with the temperature is approximately linear. Figs. 1- 3(b) show an excellent agreement between the measurements and the values predicted by Eq. (21). Here the relative discrepancies between the proposed model and the experiments are much smaller, typically below 1.5% for the cells in groups (a) and (c) and below 3% for the cells in groups (b).

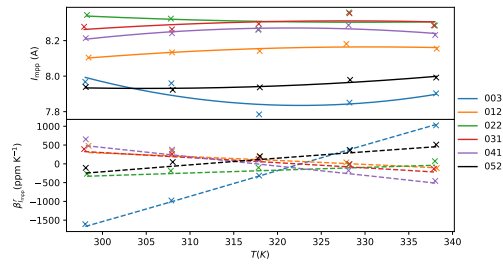
In Figs. 1- 3(c), i_{mpp} and $\beta_{i_{\text{mpp}}}^r$ are plotted as functions of the temperature. Here, a nonlinear dependence of i_{mpp} with the temperature of the cell can be observed. Moreover, in some of the measured cells, i_{mpp} appears to even have a local extremum. An example of this is the cell from position 034 in Fig. 1(c), where $i_{\text{mpp}}(T)$ is clearly observed to have a maximum. This is mirrored in the bottom figure, where it can be seen that the curve for $\beta_{i_{\text{mpp}}}^r(T)$ crosses zero. The nonlinear behavior of i_{mpp} can also be observed in Figs. 2(c) and 3(c) and it is particularly clear in cell 003 of group (b) and in cells 003 and 052 of group (c). In all three groups, the cells that show the clearest nonlinear behavior are positioned towards the top and bottom of the ingot. This may be coincidental, but it is worth noting that the concentration of impurities is higher towards the top (segregation) and bottom (diffusion) of the ingot. This suggests a connection between the nonlinear behavior of i_{mpp} and high impurity concentration. Despite the non-linear behavior of i_{mpp} , the proposed model shows a reasonably good agreement with experimental values of $\beta_{i_{\text{mpp}}}^r$ for all the studied cells. It can be concluded from Fig. 1(c) that restricting the temperature sensitivity of i_{mpp} of the studied cells to a single coefficient may be misleading. Although these nonlinearities originate, from a physical point of view, from the dependence of $\beta_{i_{\text{mpp}}}^r$ with $\beta_{i_{\text{sc}}}^r$ [3]; the nonlinear behavior of i_{mpp} can be implied from Eq. (5). If a single coefficient can describe the temperature sensitivity of V_{mpp} and P_{mpp} , then, one can write $V_{\text{mpp}} = a_1T + b_1$ and $P_{\text{mpp}} = a_2T + b_2$. Here a_i are the slopes of the straight



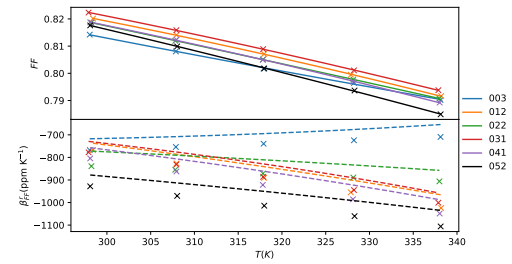
(a) V_{mpp} and $\beta_{V_{\text{mpp}}}^r$ as a function of the cell temperature.



(b) P_{mpp} and $\beta_{P_{\text{mpp}}}^r$ as a function of the cell temperature.

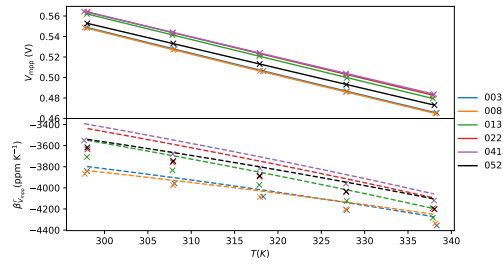


(c) i_{mpp} and $\beta_{i_{\text{mpp}}}^r$ as a function of the cell temperature.

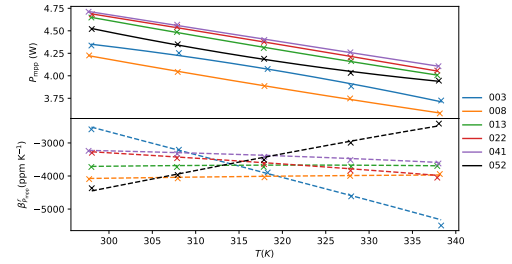


(d) FF and β_{FF}^r as a function of the cell temperature.

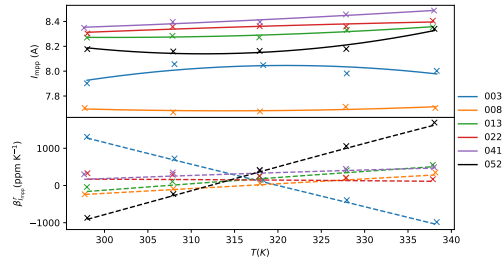
Figure 2: V_{mpp} , i_{mpp} , P_{mpp} , FF and their corresponding relative TCs as a function of the temperature for the cells in group (b).



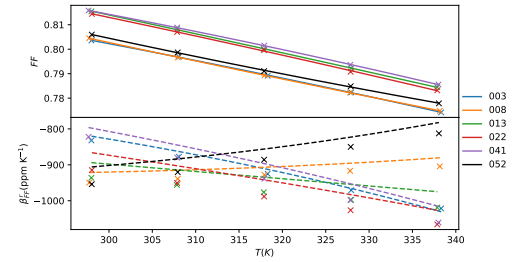
(a) V_{mpp} and $\beta_{V_{\text{mpp}}}^r$ as a function of the cell temperature.



(b) P_{mpp} and $\beta_{P_{\text{mpp}}}^r$ as a function of the cell temperature.



(c) i_{mpp} and $\beta_{i_{\text{mpp}}}^r$ as a function of the cell temperature.



(d) FF and β_{FF}^r as a function of the cell temperature.

Figure 3: V_{mpp} , i_{mpp} , P_{mpp} , FF and their corresponding relative TCs as a function of the temperature for the cells in group (c).

lines, equal to the corresponding absolute TC, i.e., $a_1 = \beta_{V_{\text{mpp}}}$ and $a_2 = \beta_{P_{\text{mpp}}}$, and b_i are the parameters in question at $T = 0$ K. Since V_{mpp} and P_{mpp} must follow Eq. (5), i_{mpp} must be given by

$$i_{\text{mpp}} = \frac{a_2 T + b_2}{a_1 T + b_1}, \quad (28)$$

which is not a linear function and, therefore, its derivative is not a constant. Therefore V_{mpp} , i_{mpp} and P_{mpp} cannot be linearly dependent on the temperature simultaneously.

Figs. 1- 3(d) show FF and β_{FF}^r plotted as functions of the temperature for the cells in groups (a), (b) and (c), respectively. Here, some small bends in the curves can be observed but, overall, the dependence with the temperature of the measurements is well described by straight lines. Here, the discrepancy between the predicted values and the experiments may also be attributed to temperature noise in the measurements and the diode model employed in the derivation of the expressions. Still, the proposed model predicts reasonably well the experimental values.

8 Conclusions

In this work, analytical expressions that describe the temperature sensitivity of the maximum power point have been derived. The expressions were tested with measurements from 18 multicrystalline silicon solar cells with different bulk resistivities and cell architectures. It was found that the new model describes with low discrepancy the temperature sensitivity of the investigated parameters and is in very good agreement with the experimental values.

From Eq. (28), it was concluded that not all parameters of a solar cell can vary linearly with the temperature at the same time. Using a single valued TC, though practical, may therefore be misleading. Additionally, it is worth noting that a single TC does not provide any information of the temperature sensitivity of the solar cell outside of the normal operating temperature interval, where linear dependence with temperature is usually assumed [3]. Contrary to previous literature, the model presented in this work shows how the temperature coefficient of solar cell parameters may vary with the temperature and, since no assumptions have been made regarding the temperature dependence of the parameters, the derived expressions describe the temperature sensitivity of the maximum power point at any given temperature. Finally, with respect to further developments, the techniques and methods employed in this work may be used to derive expressions for the TCs that include the effect of the series resistance [13, 14]. This would not only allow for a more accurate description of

the temperature sensitivity of the MPP, but also potentially gaining understanding of the temperature sensitivity of the series resistance.